

The Transient Ceiling Flows of Growing Rack Storage Fires

HONG-ZEUNG YU and PARASKEVAS STAVRIANIDIS

Factory Mutual Research Corporation
1151 Boston-Providence Turnpike
Norwood, Massachusetts 02062, USA

ABSTRACT

Transient ceiling flows induced by growing rack storage fires were investigated in the period where the convective heat release rates produced by these fires had a power-law dependence on time to the third power. Empirical correlations for the maximum excess gas temperature, maximum gas velocity, temperature profile depth, and velocity profile depth of the transient ceiling flow were established in terms of a normalized convective heat release rate of the fire and a normalized radial distance from the fire axis.

KEYWORDS: rack storage fires, transient ceiling flows, modeling and scaling

NOMENCLATURE

A	$g/(C_p T_{\infty} \rho_{\infty})$, $m^4 s^{-2} kJ^{-1}$
a	an empirical constant in Eq. (9), $kW^{1/3} m^{-5/6}$
a_T	an empirical constant in Eq. (16), $kW^{-1/3} s^{-1} m^{4/3}$
a_u	an empirical constant in Eq. (17), $kW^{-1/3} s^{-1} m^{4/3}$
b	an empirical constant in Eq. (9), $kW^{1/6} s^{1/2} m^{-2/3}$
b_T	an empirical constant in Eq. (16), $kW^{-1/6} s^{-1/2} m^{-2/3}$
b_u	an empirical constant in Eq. (17), $kW^{-1/6} s^{-1/2} m^{-2/3}$
C_p	specific heat, $kJ/kg/C$
c	an empirical constant in Eq. (12), $kW^{-2/3} s^{-2} m^{8/3}$
c_T	an empirical constant in Eq. (16)
c_u	an empirical constant in Eq. (17)
d	an empirical constant in Eq. (12), $kW^{-1/3} s^{-1} m^{-4/3}$
g	gravitational acceleration, m/s^2
H	ceiling clearance from the top of fuel array, m
Q_c	convective heat release rate, kW
Q_c^*	normalized convective heat release rate
R_c	normalized radial distance
r	radial distance, m
ΔT_m	maximum excess ceiling gas temperature, C
ΔT_m^*	normalized maximum excess ceiling gas temperature
u_m	maximum ceiling gas velocity, m/s
u_m^*	normalized maximum ceiling gas velocity
T_{∞}^m	absolute ambient temperature, K

t	time, s
t ₀	incipient time of fire growth, s
Z ₀	the virtual origin of fire plume relative to the top of fuel array, m
α	fire growth coefficient, kW s ⁻³
δ _T	temperature profile depth of the ceiling flow, m
δ _U	velocity profile depth of the ceiling flow, m
ρ _a	ambient air density, kg/m ³

INTRODUCTION

In occupancies protected by quick-response sprinklers, fire-induced ceiling gas flows prior to the first sprinkler actuation are generally highly transient, due to low gas velocity and rapid fire growth [1]. As a result, predictions of thermal responses of sprinkler links do not always warrant satisfactory results if correlations for steady ceiling flows are employed in the predictions [2]. Under this circumstance, knowledge of transient ceiling flows induced by fast growing fires is essential.

The transient ceiling flow addressed henceforth in this paper pertains to the ceiling flow induced by a growing fire. Few studies of ceiling flows of this nature have been conducted [3,4]. Heskestad developed functional relationships for maximum ceiling gas temperature, velocity and species for power-law fires [3], based on dimensional analysis of pertinent variables. Later, Heskestad and Delichatsios applied these functional relationships to wood crib fires (t² fire) [4]. Since only maximum flow properties were measured and correlated, the application of these correlations was limited to sprinklers located where maximum gas temperatures and velocities occurred. Furthermore, the correlations for power-law fires of the second power are not applicable to power-law fires with other power indices [3].

For rack storage fires, the convective heat release rates produced in the initial fire growth period have a power-law dependence on time to the third power [5]. Since transient ceiling flow correlations were not available for t³ fires, the objective of this study was to establish such correlations. In this paper, correlations for the maximum ceiling gas temperature and velocity, and the respective flow profile depths are presented.

EXPERIMENTS

A series of eight rack storage fire tests was conducted in this study. A summary of the key test variables is presented in Table I.

The fire tests were conducted in the FMRC Test Center building located at West Glocester, Rhode Island. The building's overall plan dimensions are 61 m x 76 m. Under one flat ceiling, the building consists of two approximately equal test areas, with floor-to-ceiling heights of 9.14 m and 18.28 m, respectively. The fire tests were conducted near the center of the 9.14 m area.

The fuel consisted of polystyrene cups packaged in compartmented, single-wall corrugated paper cartons. Each carton measured 0.53 m x 0.53 m x 0.51 m high and had 125 compartments in a 5 x 5 x 5 array. Vertical and horizontal cardboard dividers 0.4 mm thick were used to form the compartments, each of which contained a single 473 ml cup. Eight cartons were placed on a wood pallet forming a stack of two cartons wide by two cartons deep by two cartons high, defined as a pallet load. For each pallet load,

TABLE I. TEST VARIABLES

Test No.	No. of Tiers High	Storage* Height Above Platform (m)	Platform Height (m)	Ceiling Clearance (m)	The Beginning of Investigation Period (s)
1	2	2.93	0.3	5.91	24
2	2	2.93	0.3	5.91	27
3	3	4.48	0.3	4.36	25
4	3	4.48	0.3	4.36	25
5	4	5.95	0.3	2.89	28
6	4	5.95	0.3	2.89	21
7	5	7.50	0.3	1.34	21
8	5	7.50	0.3	1.34	28

* The vertical spacing between the horizontal rails of the steel racks was set to be 1.52 m.

the wood pallet, empty cartons with dividers and polystyrene cups weighed about 23.6 kg, 21.84 kg and 29.28 kg, respectively. The fuel array tested was two-pallet loads wide, two-pallet loads deep and two, three, four and five tiers high. A double-row steel rack was used to hold the pallet loads of fuel. An illustration of the four-tier high fuel array has been shown in Figure 1 of Ref. 6.

Measurements of ceiling gas temperatures and velocities were made at 14 stations shown in Fig. 1 (see Ref. 7 for the logic of instrumentation)

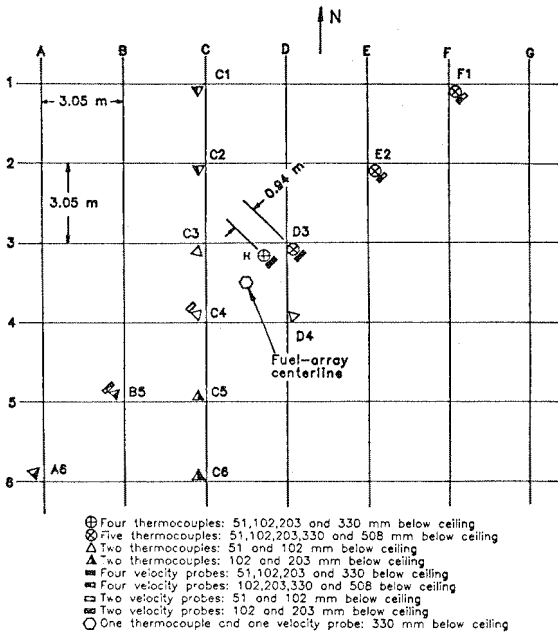


Figure 1. Instrumentation Layout.

layout). Vertical temperature and velocity profiles of the ceiling flows were measured at four stations: H, D3, E2 and F1 shown in Fig. 1. Gas temperatures were measured with 30 gauge (0.25 mm diameter), inconel-sheathed, chromel-alumel, bare bead thermocouples. Gas velocities were measured using bidirectional velocity probes.

The weight loss of the fuel array was monitored by a 3600-kg capacity, weight-measuring system (four load cells; BLH Electronic Model C3T1).

Data signals were recorded by a data acquisition system. Every second, the system scanned each data channel five times and logged the average value of the five readings on a magnetic disk.

The test procedure and the method to ignite the fuel array conformed to those described in Ref. 6. To limit fire exposure of the ceiling, the test durations for two-tier, three-tier, four-tier and five-tier fuel arrays were about 5 min, 3 min, 2 min and 1.7 min, respectively. A previous study showed that after igniting the tested fuel arrays under a 9.14 m high ceiling with a sprinkler spacing of 3.05 m by 3.05 m, the first sprinkler actuation took place within 1 min for quick response sprinklers [1]. Therefore, the ceiling flow data obtained in this study are sufficient for quick-response sprinklers.

EXPERIMENTAL RESULTS AND DATA CORRELATIONS

Convective Heat Release Rates

The convective heat release rate of the fire (Q_c) was determined from the fuel weight loss measurement (m), similar to the methodology described in Ref. 7, using the following relationship: $Q_c = mH_c$ (m), where m is the burning rate, and H_c is the convective heat generated by a unit mass of fuel consumed. The latter was found correlated with the cumulative fuel weight loss and was quantified in another series of fire tests [8].

Figure 2 presents the convective heat release rates of the fires for Tests 1 through 8. The convective heat release rate per tier is plotted versus time lapse from the end of the fire incipient period (t_0). Also shown in the figure is the data fit of the convective heat release rates previously measured under the Fire Products Collector for the same fuel arrays [5]. As shown in Fig. 2, the convective heat release rates of the fuel arrays have a third power dependence on time in their respective initial fire growth periods.

Correlation Parameters

For a fire with a power-law heat release rate such as $Q_c = \alpha (t-t_0)^3$, the maximum excess gas temperature (ΔT_m) and velocity (U_m) at a radial distance (r) from the fire axis may be written in the following functional relationships:

$$\Delta T_m^* = f_{n_T} \{ Q_c^*, R \} \quad (1)$$

and

$$U_m^* = f_{n_U} \{ Q_c^*, R \}, \quad (2)$$

respectively, where $\Delta T_m^* = A^{-1/3} g \alpha^{-1/3} (H-Z_0)^{1/3} (\Delta T_m / T_\infty)$;

$$U_m^* = A^{-1/6} \alpha^{-1/6} (H-Z_o)^{-1/3} U_m; \quad Q^* = A^{1/6} \alpha^{-1/6} (H-Z_o)^{-2/3} Q_c^{1/3};$$

and $R = r/(H-Z_o)$.

Equations (1) and (2) were obtained by modifying the functional relationships presented in Ref. 3 by referencing the ceiling height (H) to the plume virtual origin (Z_o) and replacing the time variable with Q_c . Other variables in above equations are defined in the Nomenclature.

For rack-storage fires, the plume virtual origin can be determined by the following equations [6]: $Z_o = -1.6 + 0.094 Q_c^{2/5}$ for 2-tier rack storages; and $Z_o = -2.4 + 0.095 Q_c^{2/5}$ for 3-tier and 4-tier storages. In this study, the latter equation was assumed to be applicable to 5-tier fuel storages.

For the ceiling flows investigated here, the vertical variations of excess gas temperature and velocity below the elevation of the respective maxima could be closely approximated by half Gaussian distributions [9]. The ceiling gas temperature profile depth is defined as the vertical distance measured from the elevation of the maximum gas temperature down to where the excess gas temperature is 0.37 (1/e) times the maximum value. The velocity profile depth is defined in an analogous manner. The temperature profile depth (δ_T) and the velocity profile depth (δ_u) are expected to be correlated in the following expression:

$$\delta_T \text{ or } \delta_u / (H-Z_o) = \text{fn}_{\delta_T \text{ or } \delta_u} \{ Q^*, R \}. \quad (3)$$

Analysis and Correlation of Data

A rolling time-averaging process was employed to smooth out the measurement fluctuations due to turbulence. Since the data fluctuations ranged from 1s to 3s, an averaging period of 4s was used. The average in each period was taken as the value for the mid-time in that period.

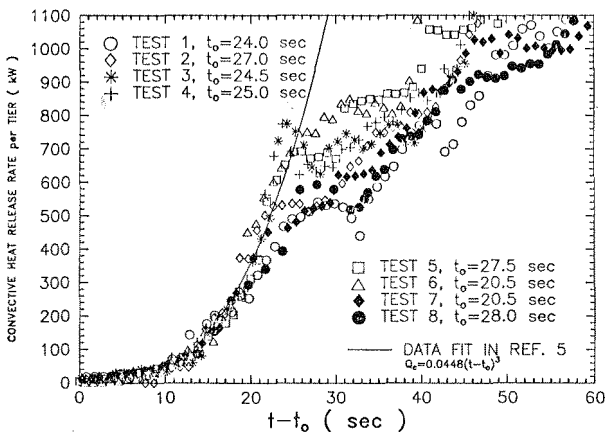


Figure 2. Convective heat release rates of Tests 1-8.

At each time instant of concern, the center of axisymmetry of the ceiling flow was determined from the gas temperatures measured at locations along the southwest-to-northeast run, and the north-to-south run, as shown in Fig. 1. The methodology to determine the fire axis location based on the spatial temperature variations had been described in Ref. 7.

The ceiling flow data of Test 6 were not employed in correlation since the flow departed severely from axisymmetry in the investigation period.

Since the location of plume virtual origin changed as the fire grew, the R value for an instrument station varied with time. In this test series, the R values for all the instrument stations ranged from 0 to 4.950 in the investigation period. At each time instant, the normalized ceiling flow data could be grouped into the following seven intervals of R values: 0.-0.16 (0.081), 0.17-0.28 (0.217), 0.30-0.50 (0.365), 0.500-1.130 (0.787), 1.190-2.500 (1.749), 2.600-3.500 (3.048) and 3.800-4.950 (4.333), where the values in the parentheses are the designated nominal values for the respective intervals. The data obtained at an instrument station may be split into two R intervals, depending on the R range at this station. In this paper, the ceiling flow data will be shown only for the following nominal R values: 0.081 (temperature and velocity only), 0.217 (flow depths only), 0.365, 1.749 and 4.333. However, the correlation equations to be presented later were established based on the entire data obtained in this study [9].

Ceiling Gas Temperature

Figure 3 presents the normalized maximum excess gas temperatures versus normalized convective heat release rates for the four selected nominal R values. Since the ambient temperature in this test series ranged from 296

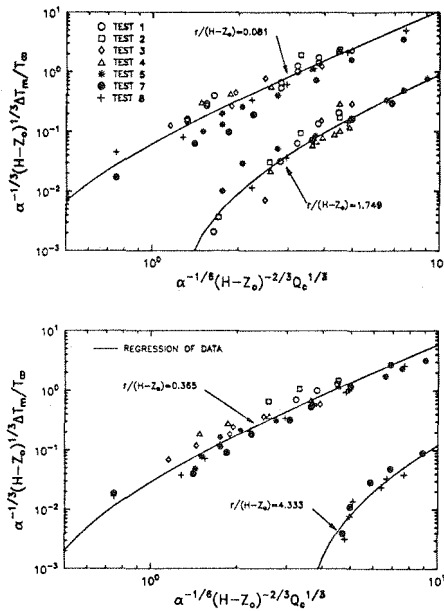


Figure 3. Correlations of maximum excess ceiling gas temperatures at $r/(H-Z_0) = 0.081, 0.365, 1.749$ and 4.333 .

to 301K, the variation of A in Eqs. (1) and (2) was negligible. As a result, A was not included in the correlation.

The equation,

$$Y_T = \left(\frac{X - b}{a} \right)^2, \quad (4)$$

where $Y_T = \alpha^{-1/3} (H-Z_0)^{1/3} \Delta T_m / T_m$ and $X = \alpha^{-1/6} (H-Z_0)^{-2/3} Q_c^{1/3}$, was employed to represent the data pertaining to the individual nominal R value. In Eq. (4), a and b are empirical constants to be determined.

For each nominal value of R, the data were correlated with Eq. (4) using the least-squares method to yield the values of a and b. These determined a and b values were fitted with the following equations:

$$a = -0.040R^4 + 0.316R^3 - 0.658R^2 + 3.991R + 3.094, \quad (5)$$

and

$$b = 0.118R^4 - 0.066R^3 + 0.090R^2 + 0.646R - 0.058, \quad (6)$$

respectively, for $0 < R < 4.95$.

Ceiling Gas Velocity

Figure 4 shows the normalized data of maximum ceiling gas velocity corresponding to the four nominal values of R indicated in the figure. The family of hyperbolic equations,

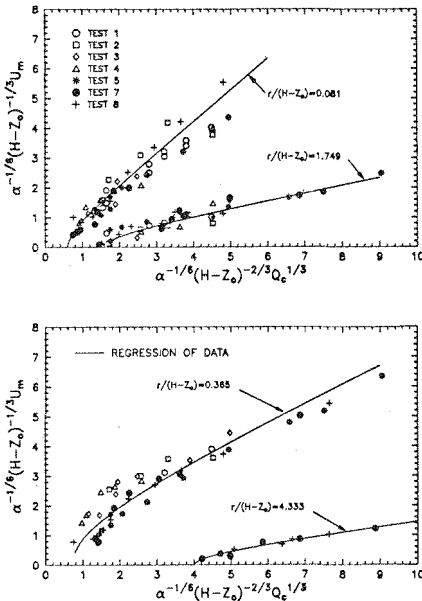


Figure 4. Correlations of maximum ceiling gas velocities at $r/(H-Z_0) = 0.081, 0.365, 1.749$ and 4.333 .

$$Y_u^2 = c (X - X_0^2) - d, \quad (7)$$

was employed to represent the gas velocity data. In Eq. (7), $Y_u = \alpha^{-1/6} (H-Z_0)^{-1/3} U_m$, and c , X_0 and d are empirical constants.

The values of c , X_0 and d for each nominal R were determined by the least-squares method and may be expressed in the following equations:

$$c = 1.0007 (1+R)^{-2.345} \text{ for } 0 \leq R < 4.950 \quad (8)$$

$$X_0 = \begin{cases} -40.342R^2 + 8.572R - 0.510 & \text{for } 0 \leq R < 0.365 \\ -0.040R^3 + 0.163R^2 + 0.935R - 2.617 & \text{for } 0.365 \leq R < 4.950; \\ & (m^{-2/3} s^{1/2} kW^{1/6}) \end{cases} \quad (9)$$

$$\text{and } d = \begin{cases} 0.411 + 1.102R & \text{for } 0 \leq R < 0.217 \\ 4.610 + 24.238R & \text{for } 0.217 \leq R \leq 0.365 \\ 1.095R^{-1.337} & \text{for } 0.365 \leq R < 4.95 \end{cases} \quad (10)$$

Ceiling Flow Depth

Figure 5 presents the normalized temperature profile depths; Figure 6 shows the normalized velocity profile depths. The ceiling flow depth at a radial distance in the investigation period underwent variations described hereinafter. Shortly after ignition, the ceiling gas temperature was low

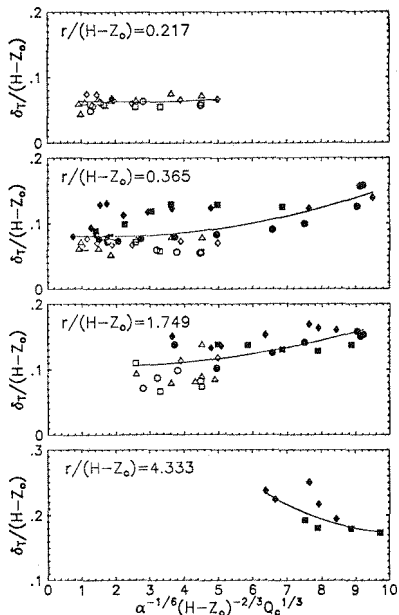


Figure 5. Correlations of ceiling gas temperature profile depths. The symbols are listed in the following: \circ Test 1; \square Test 2; \diamond Test 3; Δ Test 4; \bullet Test 5; \blacksquare Test 7; \blacklozenge Test 8; — data regression.

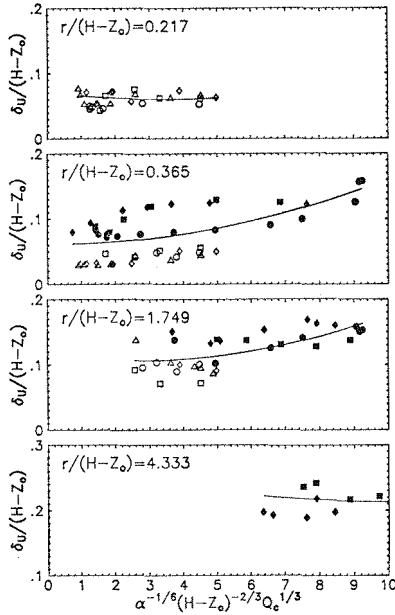


Figure 6. Correlations of ceiling gas velocity profile depths. Refer to Figure 5 for the symbols.

and flow stratification was not pronounced. In this early period, the flow depth tended to be relatively large because of the relatively free mixing between the ceiling flow gases and the ambient air. As the fire became larger, the ceiling gas temperature increased. This led to more significant gas stratification, faster gas transport under the ceiling, and consequently decrease of ceiling flow depth. As the fire grew further, the flow depth increased due to the large volume of fire gases produced and the air entrained into the plume and the ceiling flow.

The temperature profile depths at each nominal R may be expressed by the parabolic equation:

$$\delta_T/(H-Z_o) = a_T X^2 + b_T X + C_T \quad (11)$$

and similarly,

$$\delta_u/(H-Z_o) = a_u X^2 + b_u X + C_u \quad (12)$$

may be used to correlate the velocity profile depth data.

The empirical coefficients in Eq. (11) and (12) were determined by fitting the respective normalized data using the least-squares method. For $0 < R < 4.950$, the values of these coefficients may be approximated by

$$a_T = -5.326 \times 10^{-4} R^3 + 3.612 \times 10^{-3} R^2 - 5.256 \times 10^{-3} R + 2.276 \times 10^{-3}; \quad (13)$$

$$b_T = 6.910 \times 10^{-3} R^3 - 0.049 R^2 + 0.068 R - 0.019, \quad (14)$$

$$c_T = -0.010 R^3 + 0.094 R^2 - 0.102 R + 0.093, \quad (15)$$

$$a_U = 1.912 \times 10^{-5} R^3 + 9.610 \times 10^{-6} R^2 - 6.811 \times 10^{-4} R + 1.525 \times 10^{-3}, \quad (16)$$

$$b_U = -7.771 \times 10^{-4} R^4 + 7.302 \times 10^{-3} R^3 - 0.024 R^2 + 0.029 R - 0.015, \quad (17)$$

and

$$c_U = 2.119 \times 10^{-3} R^4 - 0.019 R^3 + 0.066 R^2 - 0.059 R + 0.089. \quad (18)$$

CONCLUSIONS

Empirical correlations for transient ceiling flows were established for power-law fires of the third power, which delineated the initial fire growth for high rack-storage fuel arrays investigated in this study. The maximum gas velocities and maximum excess gas temperatures in the ceiling flow were correlated with respect to two parameters: one was a normalized convective heat release rate, the other was a normalized radial distance from the fire axis.

The vertical profiles of excess gas temperature and velocity in the ceiling flow below the elevation of the maximum temperature or velocity could be closely represented by halves of Gaussian distributions [9]. The characteristic widths of these half Gaussian distributions, defined as temperature profile depths and velocity profile depths, respectively, were correlated with the same parameters used in the correlations of gas temperature and velocity data.

REFERENCES

1. Yu, H-Z., "RDD Test Protocol for Early Suppression Fast Response Sprinkler Applications," FMRC Technical Report, J.I. ON1JO.RA, 1989.
2. Walton, W.D. and Notarianni, K., "A Comparison of Ceiling Test Temperatures Measured in an Aircraft Hanger Test Fire with Temperatures Predicted by the DETACT-QS and LAVENT Computer Models," Fourth CIB Workshop on Fire Modeling, National Institute for Standards and Technology, Feb. 12-14, 1990.
3. Heskestad, G., "Similarity Relations for the Initial Convective Flow Generated by Fires," ASME Paper No. 72-WA/HT-17, 1972.
4. Heskestad, G. and Delichatsios, M.A., "The Initial Convective Flow in Fire," The Seventeenth Symposium (International) on Combustion, p. 1113, The Combustion Institute, 1978.
5. Yu, H-Z., "Transient Plume Influence in Measurement of Convective Heat Release Rates of Fast-Growing Fires Using a Large-Scale Fire Products Collector," ASME Journal of Heat Transfer, Vol. 112, p. 186-191, 1990.
6. Yu, H-Z., and Kung, H-C, "Strong Buoyant Plumes of Growing Rack Storage Fires," The Twentieth Symposium (International) on Combustion, p. 1567, The Combustion Institute, 1984.
7. Kung, H-C., Yu, H-Z, and Spaulding, R.D., "Ceiling Flows of Growing Rack Storage Fires," Twenty-First Symposium (International) on Combustion, The Combustion Institute, pp. 121-128, 1986.
8. Yu, H-Z., "Transient Plume Influence in Measurement of Rack Storage Fires," FMRC Technical Report, J.I. ON1JO.RA(2), 1989.
9. Yy, H-Z., and Stavrianidis, P., "The Transient Ceiling Flows of Growing Rack Storage Fires," FMRC Technical Report, J.I. ON1JO.RA(3), 1989.